Dyes and Pigments 83 (2009) 218–224

Contents lists available at ScienceDirect

Dyes and Pigments

journal homepage: www.elsevier.com/locate/dyepig

Phosphorescent, green-emitting Ir(III) complexes with carbazolyl-substituted 2-phenylpyridine ligands: Effect of binding mode of the carbazole group on photoluminescence and electrophosphorescence

Min Ju Cho[a], Jung-Il Jin[a], Dong Hoon Choi[a,*], Young Min Kim[b], Young Wook Park[b], Byeong-Kwon Ju[b]

[a] Department of Chemistry, Advanced Materials Chemistry Research Center, Korea University, 5 Anam-dong, Sungbuk-gu, Seoul 136-701, South Korea
[b] Display and Nanosystem Laboratory, College of Engineering, Korea University, 5 Anam-dong, Sungbuk-gu, Seoul 136-701, South Korea

ARTICLE INFO

Article history:
Received 11 February 2009
Received in revised form
29 April 2009
Accepted 29 April 2009
Available online 12 May 2009

PACS:
78.60.Fi
78.66-w
78.55

Keywords:
Iridium(III) complex
Carbazole
Solubility
Photoluminescence
Triplet energy transfer
Phosphorescence

ABSTRACT

The ligands, 9-((6-phenylpyridin-3-yl)methyl)-*9H*-carbazole and 9-(4-(pyridin-2-yl)benzyl)-*9H*-carbazole were synthesized by attaching a carbazolyl group to the pyridine and phenyl rings of 2-phenylpyridine, respectively. Ir(III) complexes were prepared by a simple procedure and the solubility of the novel complexes was significantly better than that of the conventional, green-emitting conventional *fac*-tris(2-phenylpyridinato-C^2,N)iridium(III). The Ir(III) complexes were used to prepare electrophosphorescent polymer light-emitting devices. The device comprising 10% of *fac*-tris(2-(4′-((9*H*-carbazol-9-yl)methyl)phenyl)pyridinato-C^2,N)iridium(III) exhibited an external quantum efficiency of 7.88%, luminous efficiency of 23.01 cd/A, and maximum brightness of 32,640 cd/m^2. The color of the emissions of *fac*-tris(2-(4′-((9*H*-carbazol-9-yl)methyl)phenyl)pyridinato-C^2,N)iridium(III) was similar to that of conventional *fac*-tris(2-phenylpyridinato-C^2,N)iridium(III). This work shows that integration of a rigid hole-transporting carbazole and phosphorescent complex in one molecule provides a new route to highly efficient, solution-processable complexes for electrophosphorescent applications.

1. Introduction

Electroluminescence (EL) devices using small molar mass organic materials are used in many applications such as flat-panel or flexible display devices [1–5]. Of the various kinds of light-emitting organic materials available, phosphorescent dye molecules are especially promising because both singlet and triplet excitons can generate unique light emission with a theoretical internal quantum efficiency of 100% [1,6,7]. In particular, cyclometalated Ir(III) complexes show high phosphorescent efficiencies and are one of the most important classes of phosphorescent dyes as they exhibit relatively high phosphorescent efficiencies and their ligand structures are easily modified to tune the emission color [8–13]. In an attempt to improve the formulation of optical light-emitting devices (OLEDs), we have sought to investigate novel, highly soluble materials. In this context, a dendritic architecture was considered to provide improved solubility as well as site isolation by the use of various peripheral groups around the emission center by means of a reduction in triplet–triplet annihilation between dopants [14–16]. However, significant emission spectral shifts were observed for such dendrimers and dendritic phosphorescent Ir(III) complexes [9,17,18]. By maintaining the electronic property of the original ligand, highly soluble Ir(III) complexes bearing a carbazolyl ligand through a non-conjugated alkylene spacer were produced [19].

This paper concerns two different highly soluble Ir(III) complexes bearing a carbazolyl-substituted 2-phenylpyridine ligand. By changing only the substitution position of the carbazole group, it was possible to observe fine shifts in both absorption and photoluminescent (PL) spectra. Significant improvements occurred in both the luminous efficiency and the brightness of green photoluminescent light-emitting devices (PLEDs) fabricated by doping *fac*-tris(3-((9*H*-carbazol-9-yl)methyl)-2-phenylpyridinato-C^2,N)iridium (III) (Ir(Cz-ppy)$_3$) and *fac*-tris(2-(4′-((9*H*-carbazol-9-yl)methyl)phenyl)pyridinato-C^2,N)iridium (III) (Ir(ppy-Cz)$_3$) into poly(*N*-vinylcarbazole) (PVK) blended with 5,4-*tert*-butylphenyl-1,3,4-oxadiazole (PBD), an electron transport molecule. For reference, the conventional *fac*-tris(2-phenylpyridinato-C^2,N)iridium(III)

---

* Corresponding author. Tel.: +82 2 3290 3140; fax: +82 2 924 3141.
E-mail address: dhchoi8803@korea.ac.kr (D.H. Choi).

0143-7208/$ – see front matter © 2009 Elsevier Ltd. All rights reserved.
doi:10.1016/j.dyepig.2009.04.010

($Ir(ppy)_3$) was employed to compare device performance. The emission center in $Ir(Cz\text{-}ppy)_3$ and $Ir(ppy\text{-}Cz)_3$ was observed to be fairly isolated and its properties were not much affected by the presence of a carbazolyl peripheral group.

2. Experimental

2.1. Materials

All commercially available starting materials and solvents were purchased from Aldrich, TCI, and ACROS Co. and used without further purification unless otherwise stated. HPLC grade dimethylformamide (DMF) and dichloromethane (DCM) were purchased from Samchun Chemical and distilled from CaH_2 immediately before use. All reactions were performed under an argon atmosphere unless otherwise stated. $Ir(Cz\text{-}ppy)_3$ was synthesized by following the literature method we reported recently [19].

2.2. Synthesis

2.2.1. 9-(6-Chloropyridin-3-ylmethyl)-9H-carbazole (**1**)

Sodium hydride (2.30 g, 0.055 mol) was suspended in dried dimethylformamide (DMF, 50 mL) at 0 °C. Carbazole (8.35 g, 0.05 mol) in DMF (100 mL) was added dropwise into the mother solution and the mixture was stirred for 0.5 h. Then, 1-bromo-4-(bromomethyl)benzene (12.5 g, 0.05 mol) in DMF (100 mL) was also added dropwise and the reaction mixture was stirred constantly at room temperature for 3 h. Finally, the reaction mixture was poured into 100 mL of water and neutralized with aqueous 2 M HCl. After filtration of the solution, the crude product was obtained and purified by silica-gel column chromatography (chloroform as eluent) to give a white powder in 90.4% yield (15.21 g, 0.045 mol).

^1H NMR (400 MHz, $CDCl_3$) δ 8.14 (d, $J = 8.0$ Hz, 2H), 7.43 (t, $J = 8.0$ Hz, 2H), 7.37 (d, $J = 8.0$ Hz, 2H), 7.30 (d, $J = 8.0$ Hz, 2H), 7.27 (t, $J = 8.0$ Hz, 2H), 6.99 (d, $J = 8.0$ Hz, 1H), 5.44 (s, 2H). FABMS: m/z 335.0325 (M^+). Anal. calcd for $C_{19}H_{14}BrN$: C, 67.87; H, 4.20; N, 4.17. Found: C, 67.71; H, 4.26; N, 4.24.

2.2.2. 4-((9H-Carbazol-9-yl)methyl)phenylboronic acid (**2**)

To a stirred solution of compound **1** (6.72 g, 0.02 mol) in dry THF (100 mL) under argon, a solution of 2.5 M *n*-butyllithium (*n*-BuLi) in hexane (8.0 mL, 0.02 mol) was added dropwise at −78 °C. The mixture was stirred at this temperature for 1 h to form a white suspension. Trimethylborate (2.08 g, 0.02 mol) was added and the mixture was allowed to warm up to room temperature. A solution of conc. HCl (10 ml) in ice-cold water (100 ml) was added to the white suspension. The organic phase was separated by ethyl ether (200 mL) and washed with brine before drying over anhydrous Na_2SO_4. The solvent was evaporated and the crude product was purified by chloroform to afford **2** as a white solid (4.21 g, 0.014 mol, 70%).

^1H NMR (400 MHz, DMSO-d_6) δ 8.18 (d, $J = 8.0$ Hz, 2H), 7.98 (s, 2H), 7.66 (d, $J = 8.0$ Hz, 2H), 7.61 (d, $J = 8.0$ Hz, 2H), 7.42 (t, $J = 8.0$ Hz, 2H), 7.21 (t, $J = 8.0$ Hz, 2H), 7.12 (d, $J = 8.0$ Hz, 1H), 5.66 (s, 2H). FABMS: m/z 301.1252 (M^+). Anal. calcd for $C_{19}H_{16}BNO_2$: C, 75.78; H, 5.36; N, 4.65. Found: C, 75.65; H, 5.23; N, 4.58.

2.2.3. 9-(4-(Pyridin-2-yl)benzyl)-9H-carbazole (**3**)

A solution of 2-bromopyridine (1.58 g, 0.01 mol) and tetrakis (triphenylphosphine) palladium(0) ($Pd(PPh_3)_4$, 0.21 g, 0.18 mmol) in toluene (100 mL) was treated with a degassed solution of K_2CO_3 (3.9 g, 0.024 mol) in H_2O (30 mL), followed by addition of the solution of **2** (3.01 g, 0.01 mol) in ethanol (20 mL). The mixture was stirred at 85 °C overnight under Ar gas. After cooling, the reaction mixture was poured into 100 mL of water and extracted with toluene. The combined organic layers were washed with brine and dried over Na_2SO_4. Removal of the solvent under reduced pressure gave a crude product, which was purified by silica-gel column chromatography (eluent ethyl acetate/chloroform, 1:15) to give a white powder in 75% yield (2.51 g, 7.5 mmol).

^1H NMR (400 MHz, $CDCl_3$) δ 8.66 ~8.68 (m, 1H), 8.16 (d, $J = 8.0$ Hz, 2H), 7.89 (d, $J = 8.0$ Hz, 2H), 7.70 (t, $J = 8.0$ Hz, 2H), 7.63 (d, $J = 8.0$ Hz, 2H), 7.45 (t, $J = 8.0$ Hz, 2H), 7.39 (d, $J = 8.0$ Hz, 2H), 7.28 (t, $J = 8.0$ Hz, 2H), 7.25 (d, $J = 8.0$ Hz, 2H), 719–7.22 (m, 1H), 5.58 (s, 2H). FABMS: m/z 335.1540 ($(M + H)^+$). Anal. calcd for $C_{24}H_{18}N_2$: C, 86.20; H, 5.43; N, 8.38. Found: C, 86.14; H, 5.52; N, 8.45.

2.2.4. $Ir(ppy\text{-}Cz)_3$ (**4**)

To a mixed solvent (2-ethoxyethanol/H_2O, 3:1, 60 mL) of **3** (1.67 g, 5.0 mmol) was added $IrCl_3 \cdot 3H_2O$ (0.88 g, 2.5 mmol) and the reaction mixture was heated to 120 °C for 24 h. The resulting solution was concentrated and the crude solid was collected and washed with 100 mL of water, 50 mL of hexane, and 50 mL of ethyl ether, sequentially. The crude product was purified by silica-gel column chromatography (CH_2Cl_2) to give a yellow powder (Ir(III)-dimer) in 74% yield (1.65 g, 0.92 mmol).

To a 2-ethoxyethanol (15 mL) solution of Ir(III)-dimer (1.23 g, 0.69 mmol) were added **3** (0.53 g, 1.60 mmol) and excess K_2CO_3, and the reaction mixture was heated to 120 °C for 12 h. After cooling to room temperature, a dark yellowish precipitate was filtered off and washed with 200 mL of methanol/ethyl ether (1:1, v/v). The crude product was purified by silica-gel column chromatography (eluent hexane/dichloromethane, 1:5) to give a white yellow powder in 50% yield (0.82 g, 0.72 mmol).

^1H NMR (400 MHz, $CDCl_3$) δ 8.05 (d, $J = 8.0$ Hz, 6H), 7.69 (d, $J = 8.0$ Hz, 3H), 7.48 (t, $J = 8.0$ Hz, 6H), 7.39 (d, $J = 8.0$ Hz, 3H), 7.25 ~ 7.30 (m, 12H), 7.14 (t, $J = 8.0$ Hz, 6H), 6.82 (s, 3H), 6.78 (t, $J = 8.0$ Hz, 3H), 6.56 (d, $J = 8.0$ Hz, 3H), 5.06 ~ 5.19 (m, 6H). ^{13}C NMR (125 MHz, $CDCl_3$) δ 166.291, 161.515, 147.307, 143.297, 140.916, 138.365, 136.133, 136.081, 125.733, 124.401, 123.070, 122.058, 120.302, 118.867, 118.852, 109.389, 47.324. FABMS: m/z 1193.4 ($(M + H)^+$). Anal. calcd for $C_{72}H_{51}IrN_6$: C, 72.52; H, 4.31; N, 7.05. Found: C, 72.45; H, 4.34; N, 7.12.

2.3. Characterization

^1H NMR spectra were recorded on a Varian Mercury NMR 400 MHz spectrometer using deuterated chloroform purchased from Cambridge Isotope Laboratories, Inc. ^{13}C NMR spectra were recorded using a Varian Inova-500 spectrometer. Elemental analysis was performed by using an EA1112 (Thermo Electron Corp.) elemental analyzer. Mass analysis was performed on a JMS-AX505WA (JEOL) mass spectrometer.

2.4. Absorption and photoluminescence spectroscopy

Absorption spectra of chloroform solutions were obtained using a UV–vis spectrometer (HP 8453, PDA type) in the wavelength range of 190–1100 nm. PL spectra were recorded with a Hitachi F-7000 FL spectrophotometer.

2.5. Electroluminescence measurement

The multilayer diodes have a structure of ITO/PEDOT:PSS (40 nm)/PVK with Ir(III) complex (40 nm)/BCP (5 nm)/Alq_3 (35 nm)/LiF (1 nm)/Al (100 nm), respectively. The conducting PEDOT:PSS layer was spin-coated onto the ITO-coated glasses in an argon atmosphere. The emitting PVK/Ir complex layer then was spin-coated onto the thoroughly dried PEDOT layer using the solution (conc. 1.5 wt%) in monochlorobenzene.

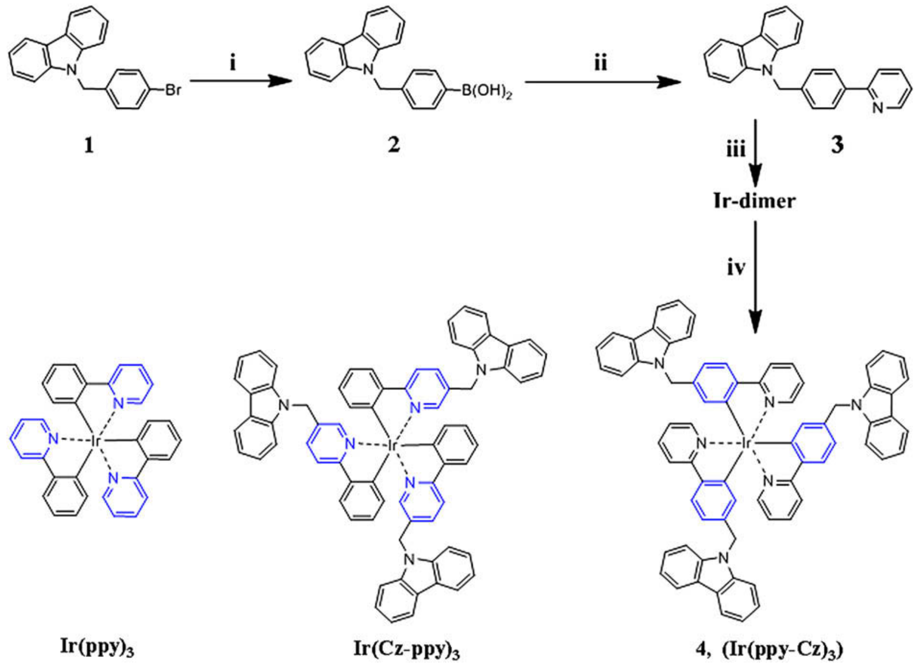

Scheme 1. Synthetic procedure: (i) *n*-BuLi, $B(OCH_3)_3$, HCl, (ii) 2-bromopyridine, $Pd(PPh_3)_4$, K_2CO_3, toluene/H_2O/EtOH, 80 °C, (iii) $IrCl_3 \cdot 3H_2O$, 2-ethoxyethanol, H_2O, 120 °C, (iv) compound 3, K_2CO_3, 2-ethoxyethanol, 120 °C.

For multilayer devices, the 2,9-dimethyl-4,7-diphenyl-1,10-phenanthroline (BCP) and tris(8-hydroxyquinoline) aluminium (Alq_3) layer were vacuum-deposited onto the emitting polymer layer. Finally, LiF (1 nm)/Al (100 nm) electrodes were deposited onto the Alq_3 layer. The EL characteristics were measured using a PR-670 SpectraScan spectroradiometer (Photo Research, Inc.) and the Model 237 High-Voltage Source-Measure Unit (Keithley Instruments, Inc.) in a dark box and air atmosphere. The CIE 1931 color coordinate was automatically calculated by the PR-670. Assuming that the light source was lambertian, the current, power, and quantum efficiencies were calculated from the measured data.

3. Results and discussion

3.1. Synthesis of carbazole-substituted Ir(III) complex

The synthetic route to the Ir(III) complex containing carbazolyl substituent is depicted in Scheme 1 including the structures of $Ir(ppy)_3$ and $Ir(Cz\text{-}ppy)_3$. A carbazolyl group was tethered to 2-phenylpyridine in two different modes. In $Ir(Cz\text{-}ppy)_3$ [19], it was attached to the 5-position of the pyridine ring; in $Ir(ppy\text{-}Cz)_3$, it was tethered to the 4-position of the phenyl ring. 2-Chloro-5-chloromethyl-pyridine was first reacted with carbazole and the new carbazole-substituted ligand was synthesized using 9-(6-chloropyridin-3-ylmethyl)-9*H*-carbazole via the Suzuki coupling reaction in a moderately good yield of $Ir(Cz\text{-}ppy)_3$ (>90%). When preparing $Ir(ppy\text{-}Cz)_3$, a different synthetic route was followed. After synthesizing 4-((9*H*-carbazol-9-yl)methyl)phenylboronic acid, 2-bromopyridine was also reacted through Suzuki coupling to yield a 9-(4-(pyridin-2-yl)benzyl)-9*H*-carbazole ligand.

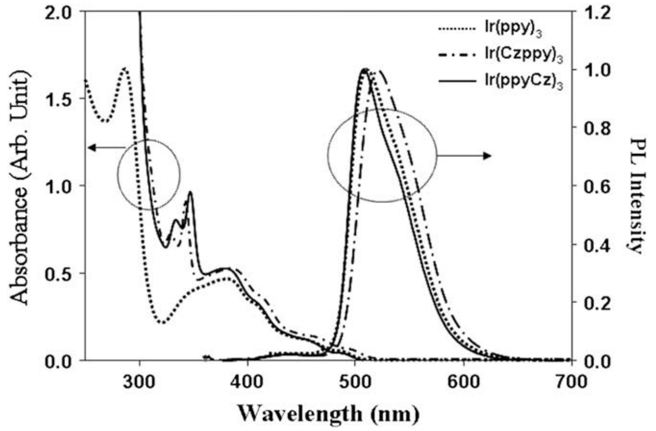

Fig. 1. UV–vis absorption and PL spectra of $Ir(ppy)_3$, $Ir(Cz\text{-}ppy)_3$, and $Ir(ppy\text{-}Cz)_3$ in the solution state (chloroform).

Following the Nonoyama reaction, $IrCl_3 \cdot 3H_2O$ was treated with an excess of carbazolyl phenylpyridyl ligands in a mixed solvent of 2-ethoxyethanol and water (3:1, v/v) to form an iridium dimer with chloride bridges. Then, the chloride-bridged dimer was converted to $Ir(Cz\text{-}ppy)_3$ in a weak basic condition. Every phenylpyridine ligand acquired one carbazole substitute. In order to ensure solubility, the carbazole group was attached to the main ligand through an alkylene spacer. A significant improvement in the solubility of the iridium complex was observed only on introducing the carbazolyl moiety into the conventional ligand in $Ir(ppy)_3$. The miscibility improvement also arises from the better compatibility of the

Table 1
Measured physical parameters of $Ir(ppy)_3$, $Ir(Cz\text{-}ppy)_3$, and $Ir(ppy\text{-}Cz)_3$.

Ir(III) complex	Absorption wavelength (nm)	λ_{em} (nm) (FWHM)[a]	E_{ox}[b] (V)	E_g[c] (eV)	HOMO[d] (eV)	LUMO[e] (eV)
$Ir(ppy)_3$	286, 406, 452, 481	510 (60)	0.76	2.45	−5.16	−2.71
$Ir(Cz\text{-}ppy)_3$	343, 384, 412, 461, 493	520 (62)	0.74	2.40	−5.14	−2.74
$Ir(ppy\text{-}Cz)_3$	346, 378, 406, 452, 484	508 (57)	0.71	2.45	−5.11	−2.66

[a] FWHF, full width at half maximum.
[b] Oxidation potentials measured by cyclic voltammetry.
[c] E_g estimated from the UV–vis absorption spectra.
[d] HOMO = (E_{ox} + 4.4 eV).
[e] LUMO = HOMO + E_g.

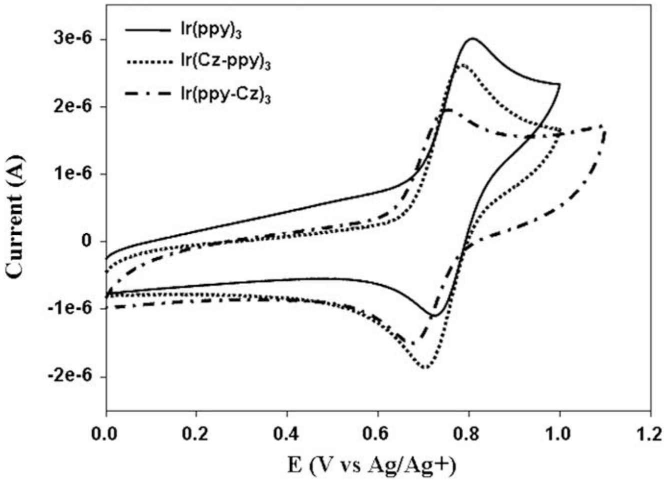

Fig. 2. Cyclic voltammograms of Ir(ppy)$_3$, Ir(Cz-ppy)$_3$ and Ir(ppy-Cz)$_3$.

carbazole-substituted Ir(III) complex with PVK. Improved solubility and miscibility with the host polymer are quite beneficial for solution processing of PLED, which leads to a more homogeneous film.

3.2. UV–vis absorption and photoluminescent properties of Ir(III) complexes

The absorption and photoluminescent (PL) spectra of the solution samples of Ir(ppy)$_3$, Ir(Cz-ppy)$_3$, and Ir(ppy-Cz)$_3$ are shown in Fig. 1. The spectral shapes were similar to that observed for Ir(ppy)$_3$ except that the spectra of Ir(ppy-Cz)$_3$ and Ir(Cz-ppy)$_3$ exhibit absorption bands at 343–347 nm. The absorption bands of the spectra of two carbazolyl-Ir(III) complexes below 320 nm are ascribed to the intra-ligand $\pi-\pi^*$ transitions originating from the Ir complex, while the absorption at around 343 nm is due to the carbazole moieties. In a lower energy region spanning from 380 to 520 nm, we could observe weak and broad absorption bands with shoulders, which can be attributed to spin-allowed and spin-forbidden metal-to-ligand charge transfer (MLCT) transitions of the Ir(III) complexes. The same feature of MLCT transition observed in three absorption spectra indicates that there was no interaction between Ir complex and pendent carbazole. There is no additional transition at lower energy (>500 nm), which can be attributed to the non-conjugated tethering of the phenylpyridine and carbazole groups in the ligand. The PL spectra of the Ir(III) complexes in $CHCl_3$ solutions are shown in Fig. 1. The emission maximum of Ir(Cz-ppy)$_3$ was observed at 520 nm in the solution state compared to 510 and 508 nm for Ir(ppy)$_3$ and Ir(ppy-Cz)$_3$, respectively. The peak emission wavelength of Ir(Cz-ppy)$_3$ is bathochromically shifted relative to that of Ir(ppy)$_3$ by ca 10 nm. It can be considered that the similar excited and ground states were involved in the phosphorescent transition of Ir(ppy)$_3$ and Ir(ppy-Cz)$_3$. Briefly, tethering the carbazole substituent to the Ir(III) complex unit *via* non-conjugated alkylene spacer does not affect the optical properties significantly. Particularly, the full width at half maximum (FWHM) of the emission spectrum of Ir(ppy-Cz)$_3$ is relatively smaller to exhibit better color homogeneity (see Table 1).

3.3. Electrochemical analysis

Electrochemical analysis was performed to determine the redox ionization potentials of the synthesized compounds. The oxidation and reduction potentials are closely related to the HOMO and LUMO levels of the analyzed compounds. Cyclic voltammograms were recorded in a solution sample, and the potentials were obtained relative to an internal ferrocene reference (Fc/Fc$^+$). Ir(ppy)$_3$, Ir(Cz-ppy)$_3$, and Ir(ppy-Cz)$_3$ in dichloromethane have reversible oxidation ($E_{ox}^{1/2}$) at 0.76, 0.74 and 0.71 V, respectively (see Table 1, Fig. 2). Unfortunately, the reduction potentials were irreversible; therefore, we were unable to estimate their LUMO energies accurately. The HOMO levels of Ir(ppy)$_3$, Ir(Cz-ppy)$_3$, and Ir(ppy-Cz)$_3$ were determined to be almost -5.16, -5.14 and -5.11 eV, respectively. In order to determine the LUMO levels, we combined the oxidation potential in CV with the optical energy band gap (E_g) resulting from the absorption edge in an absorption spectrum (see Table 1). Resulting from the triplet states of Ir(III) complexes, it can be expected that triplet–triplet energy transfer from PVK ($T_1 = 2.50$ eV) to Ir(III) complexes synthesized in this study *via* the Dexter mechanism were accompanied by efficient singlet–singlet energy transfer. It should be pointed out that the triplet state of Ir(ppy-Cz)$_3$ is identical to that of that of Ir(ppy)$_3$, which implies that almost the same excited species will be responsible for emission behaviour.

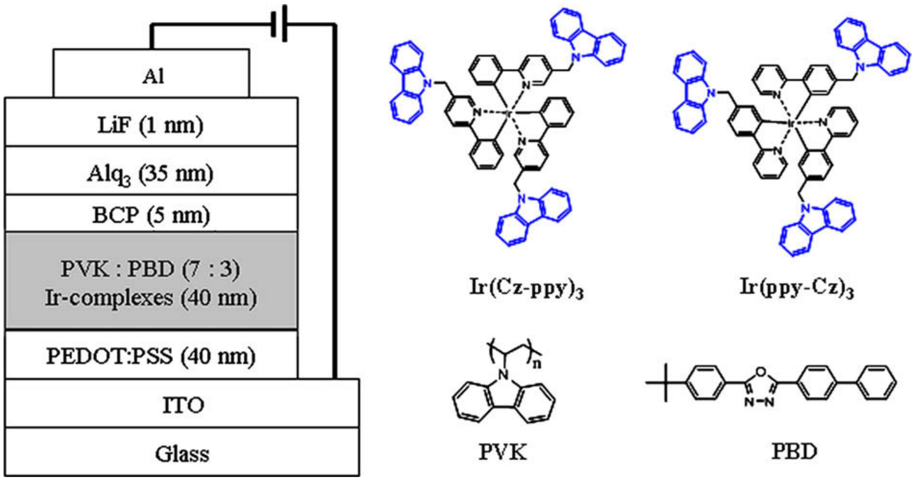

Fig. 3. Molecular structures of Ir(Cz-ppy)$_3$, Ir(ppy-Cz)$_3$, PVK, and PBD. The device configuration of electrophosphorescent PLED.

Table 2
Measured parameters of electrophosphorescent devices.

Devices	Turn-on (V)	L_{max} (cd/m^2) (J) [a]	LE$_{max}$ (cd/A) (J) [a]	PE$_{max}$ (lm/W) (J) [a]	EQE$_{max}$ (%) (J) [a]	EL λ_{max} [b] (nm) (FWHM) [c]	CIE coordinate [b] (x,y)
Device A	4	12,630(201.98)	10.62(16.22)	3.93(4.26)	3.71(2.67)	512(74)	0.31, 0.60
Device B	4.5	16,670(241.98)	15.71(5.15)	5.48(5.15)	5.32(5.15)	526(82)	0.36, 0.59
Device C	5	15,770(345.86)	11.21(3.85)	4.51(1.19)	3.80(3.85)	512(72)	0.31, 0.60
Device D	5	20,250(201.87)	19.24(1.40)	7.55(1.40)	8.68(1.40)	522(76)	0.35, 0.60
Device E	5	32,640(272.26)	23.01(9.59)	8.79(9.59)	7.88(2.30)	512(66)	0.30, 0.61

[a] Corresponding J (mA/cm^2).
[b] At 10,000 cd/m^2.
[c] FWHF, full width at half maximum.

3.4. Electrophosphorescent properties

The multilayer diodes have a structure of ITO/PEDOT:PSS (40 nm)/PVK (or PVK:PBD) with Ir(III) complex (40 nm)/BCP (5 nm)/Alq$_3$ (35 nm)/LiF (1 nm)/Al (100 nm), respectively (see Fig. 3). PVK (M_w ~ ~90,000, ACROS Co.) was selected as the polymer host. We fabricated five different multilayered devices. Devices A, B, and C were fabricated using Ir(ppy)$_3$ (6 wt%), Ir(Cz-ppy)$_3$ (10 wt%), and Ir(ppy-Cz)$_3$ (10 wt%) doped into PVK only. Devices D and E were fabricated by doping Ir(Cz-ppy)$_3$ (10 wt%), and Ir(ppy-Cz)$_3$ (10 wt%) into a PVK:PBD (70:30 wt ratio) host. Due to steric hindrance by the carbazole groups, these complexes can be employed at high concentrations in devices without incurring significant concentration quenching of PL. There is a good overlap between the PL spectrum of PVK or PVK:PBD (30 wt%) and the MLCT absorption bands of iridium complexes [12,20]. This overlap should enable efficient energy transfer from the singlet-excited state in the host to the MLCT band of the guest. Performance data of the devices are summarized in Table 2. The current density–voltage luminance curves of the five devices are shown in Fig. 4. Turn-on voltages for these devices are typical for Ir(III) complex doped PLEDs, falling in the 4.0–5.0 V range.

The maximum brightness of the LEDs was around 12,630 cd/m^2 (at 201.98 mA/cm^2) for device A, 16,670 cd/m^2 (at 241.98 mA/cm^2) for device B, and 15,770 cd/m^2 (at 345.86 mA/cm^2) for device C. Devices D and E made of the PVK:PBD host exhibited significantly increased brightness. Device E showed the highest brightness at around 32,640 cd/m^2, which is more than twice that of device C (L_{max} = 15,770 cd/m^2).

Fig. 5 displays the dependence of the luminous efficiency and external quantum efficiency on the current density for five electrophosphorescent devices. The maximum luminous efficiencies of devices A, B, and C were determined as 10.62 cd/A (at 16.22 mA/cm^2, η_{EQE} = 3.71% at 2.67 mA/cm^2), 15.71 cd/A (at 5.15 mA/cm^2, η_{EQE} = 5.3%), and 11.21 cd/A (at 3.85 mA/cm^2, η_{EQE} = 3.80%), respectively. It should be pointed out that the triplet state of PVK (T_1 = 2.50 eV) was higher in energy than that of the Ir(Cz-ppy)$_3$ (T_1 = 2.41 eV) and the Ir(ppy-Cz)$_3$ (T_1 = 2.44 eV). Interestingly, the triplet energy level of Ir(ppy-Cz)$_3$ was well matched with that of Ir(ppy)$_3$. There was a subtle difference between the efficiencies of the three samples, which cannot be explained using the molecular energy levels. Since the experiment was carried out at 298 K, an energy difference less than 0.03 eV, which is the thermal energy associated with room temperature (RT), does not completely determine the efficiency of energy transfer. It can be conjectured that the PL efficiency of carbazolyl-Ir(III) complexes could be higher than that of Ir(ppy)$_3$ because of the site-isolation effect. Qualitatively, the higher efficiency in devices B and C than device A results from the fact that carbazole units are included in the chemical structure of the ligand to improve the hole transport property and charge trapping across the multilayered devices can be facilitated [21–23].

It is well known that PVK is a blue-emitting material with good hole-transporting properties [24] and is blended with PBD to enable a balance between electron and hole-transporting properties [25,26]. When new Ir(III) complexes were doped into the PVK:PBD host, the device parameters in devices D and E were significantly enhanced compared with those in the PVK host. It is notable that the luminous efficiency (19.24 and 23.01 cd/A) and EQE (8.68 and 7.88%) of devices D and E were significantly higher than those of devices A, B and C. This can be attributed to the fact that electron transport was highly facilitated to exhibit balanced emission in the emission layer. Although space charge buildup is not so significant due to the trapping of holes on the Ir(III) complex, it is largely inhibited by supplying a sufficiently large number of electrons *via* efficient injection and transport. The holes trapped on the Ir(III) emitter are effectively neutralized *via* efficient electron injection and transport, followed by recombination of electrons in

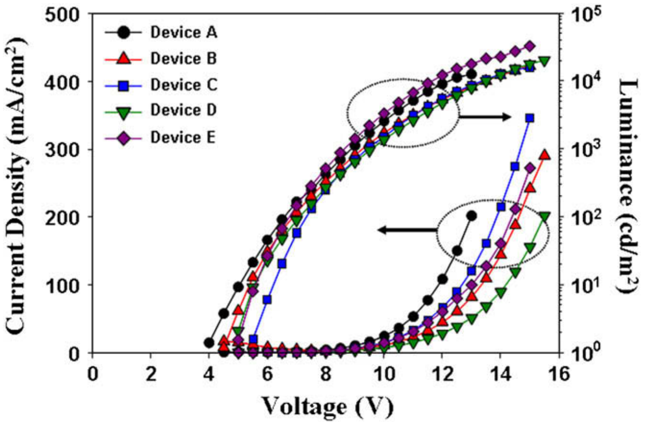

Fig. 4. Dependence of current density and luminance on the applied voltage.

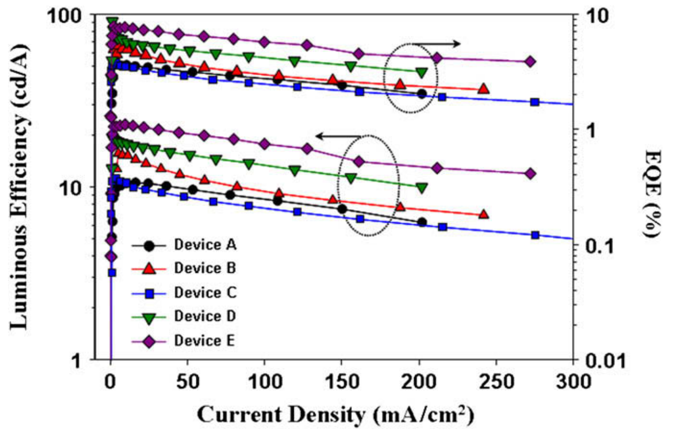

Fig. 5. Dependence of luminous efficiency and external quantum efficiency on the current density.

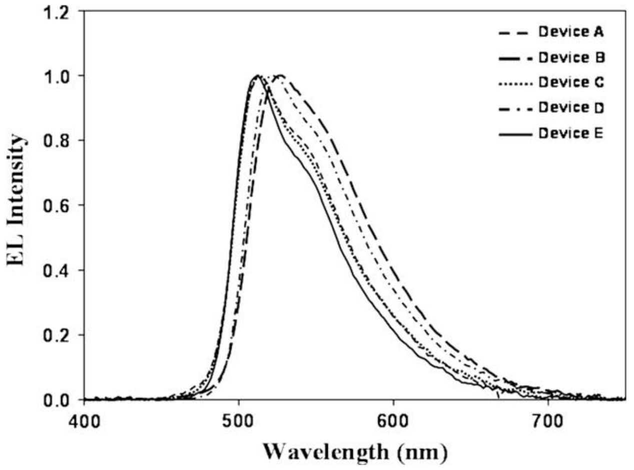

Fig. 6. EL spectra of five devices.

devices D and E. Well-balanced charge-carrier injection and transport and confinement of the emissive triplet excitons within the emission layer could be achieved, resulting in significantly improved device efficiency. Due to the presence of a carbazolyl peripheral moiety, the present device has a much slower decrease in efficiency with an increase in current density, thereby suppressing triplet–triplet annihilation.

Fig. 6 shows the EL emission spectra of the five devices. The spectra of the five devices are quite similar to the PL solution spectra of each Ir(III) complex (see Fig. 1). This suggests that the same excited state species is responsible for both the PL and EL emissions, resulting from the triplet emission due to Ir(III) complex. EL emission is dominated by the Ir(III) complex emission peak at around 512–526 nm. No host emission was observed in the fabricated devices. This seems to indicate that energy transfer from the PVK or PVK:PBD host to three Ir(III) complexes is quite efficient at the dopant concentration that was optimized in the experiment. The full width at half maximum (FWHM) is relatively smaller to exhibit better color purity, which is well consistent with that of the PL spectrum (see Fig. 1 and Table 2).

The effect of 9-((6-phenylpyridin-3-yl)methyl)-9*H*-carbazole ligand on the spectral shift to a longer wavelength induced a variation in the green emission color. The synthetic strategy to tether the carbazolyl group to the 4-phenyl ring in the 2-phenylpyridine ligand successfully tuned the color coordinate, which was matched to device A bearing Ir(ppy)$_3$ (see Fig. 7 and Table 2). This can be explained in greater detail by using the differences in the electronic properties of 9-((6-phenylpyridin-3-yl)methyl)-9*H*-carbazole and 9-(4-(pyridin-2-yl)benzyl)-9*H*-carbazole ligands.

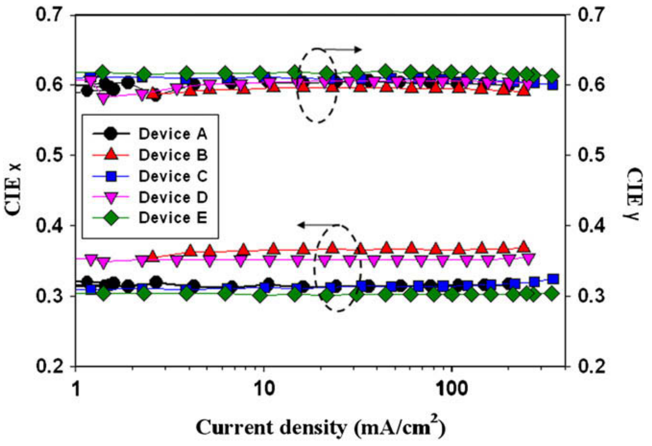

Fig. 7. Stability of the chromaticity depicted by CIE coordination.

In Fig. 7, the current density dependence of the chromaticity is shown for evaluating its stability. When the EL spectrum was converted into chromaticity coordinates on the CIE 1931 diagram, we could observe an evident stability of chromaticity with the increase in the applied voltage, concomitantly with the increase in the current density. Therefore, the stability of the color coordinate was also improved by introducing the electron transport molecule as a guest molecule into the host matrix.

4. Conclusions

This study demonstrates the new phosphorescent iridium complexes, Ir(Cz-ppy)$_3$ and Ir(ppy-Cz)$_3$, and the performance of the electrophosphorescence devices with and without PBD. The materials had dramatically increased solubility over Ir(ppy)$_3$, thus possessing great processability. In particular, the efficiency of device E (Ir(ppy-Cz)$_3$ in PVK:PBD) was significantly improved compared with other similar, conventional devices. The color coordinate of device E also compared well with that of device A with Ir(ppy)$_3$. The measurement of accurate triplet energy levels of the new Ir(III) complexes is in progress. This will provide clear information to explain the significant improvement of EL efficiency in detail. Although the performance of PLED fabricated using a solution technique is inferior to that of the device made using the vacuum deposition technique, Ir(ppy-Cz)$_3$ in PVK:PBD exhibited quite promising data for future device fabrication. Our work unambiguously demonstrates the new highly soluble Ir(III) complexes, which take advantage of efficient excited energy transfer, can be fully utilized for fabricating better phosphorescent EL devices.

Acknowledgments

This research work was supported by LG display (2009–2010). Particularly, Prof. D. H. Choi is grateful for financial support from the Seoul R&BD Program (2008–2009), and the second stage of the Brain Korea 21 Project in 2009 (Korea Research Foundation).

References

[1] Adachi C, Baldo MA, Thompson ME, Forrest SR. Nearly 100% internal phosphorescence efficiency in an organic light-emitting device. Journal of Applied Physics 2001;90:5048–51.
[2] Hong Z, Liang C, Li R, Li W, Zhao D, Fan D, et al. Rare earth complex as a high-efficiency emitter in an electroluminescent device. Advanced Materials 2001;13:1241–5.
[3] Sun PP, Duan JP, Shih HT, Cheng CH. Europium complex as a highly efficient red emitter in electroluminescent devices. Applied Physics Letters 2002;81:792–4.
[4] Liang F, Zhou Q, Cheng Y, Wang L, Ma D, Jing X, et al. Oxadiazole-functionalized europium(III) β-diketonate complex for efficient red electroluminescence. Chemistry of Materials 2003;15:1935–7.
[5] Sun PP, Duan JP, Lih JJ, Cheng CH. Synthesis of new europium complexes and their application in electroluminescent devices. Advanced Functional Materials 2003;13:683–91.
[6] Wilde AP, King KA, Watts RJ. Resolution and analysis of the components in dual emission of mixed-chelate/ortho-metalate complexes of iridium(III). Journal of Physical Chemistry 1991;95:629–34.
[7] Bernhard S, Barron JA, Houston PL, Abruña HD, Ruglovksy JL, Gao X, et al. Electroluminescence in ruthenium(II) complexes. Journal of the American Chemical Society 2002;124:13624–8.
[8] Tsutsui T, Yang M-J, Yahiro M, Nakamura K, Watanabe T, Tsuji T, et al. High quantum efficiency in organic light-emitting devices with iridium-complex as a triplet emissive center. Japanese Journal of Applied Physics 1999;38:L1502–4.
[9] Ostrowski JC, Robinson MR, Heeger AJ, Bazan GC. Amorphous iridium complexes for electrophosphorescent light emitting devices. Chemical Communications 2002:784–5.
[10] Duan JP, Sun PP, Cheng CH. New iridium complexes as highly efficient orange-red emitters in organic light-emitting diodes. Advanced Materials 2003; 15:224–8.

[11] Beeby A, Bettington S, Samuel IDW, Wang Z. Tuning the emission of cyclometalated iridium complexes by simple ligand modification. Journal of Materials Chemistry 2003;13:80–3.

[12] Gong X, Robinson MR, Ostrowski JC, Moses D, Bazan GC, Heeger AJ. High-efficiency polymer-based electrophosphorescent devices. Advanced Materials 2002;14:581–5.

[13] Ikai M, Tokito S, Sakamoto Y, Suzuki T, Taga Y. Highly efficient phosphorescence from organic light-emitting devices with an exciton-block layer. Applied Physics Letters 2001;79:156–8.

[14] Freeman AW, Koene SC, Malenfant PRL, Thompson ME, Fréchet JMJ. Dendrimer-containing light-emitting diodes: toward site-isolation of chromophores. Journal of the American Chemical Society 2000;122:12385–6.

[15] Lo S-C, Namdas EB, Shipley CP, Markham JPJ, Anthopolous TD, Burn PL, et al. The synthesis and properties of iridium cored dendrimers with carbazole dendrons. Organic Electronics 2006;7:85–98.

[16] Namdas EB, Ruseckas A, Samuel IDW, Lo S-C, Burn PL. Photophysics of *fac*-tris(2-phenylpyridine) iridium(III) cored electroluminescent dendrimers in solution and films. Journal of Physical Chemistry B 2004;108:1570–7.

[17] Lo S-C, Anthopoulos TD, Namdas EB, Burn PL, Samuel IDW. Encapsulated cores: host-free organic light-emitting diodes based on solution-processible electrophosphorescent dendrimers. Advanced Materials 2005;17:1945–8.

[18] You Y, An C-G, Lee D-S, Kim J-J, Park SY. Silicon-containing dendritic tris-cyclometalated Ir(III) complex and its electrophosphorescence in a polymer host. Journal of Materials Chemistry 2006;16:4706–13.

[19] Cho MJ, Kim JI, Hong CS, Kim YM, Park YW, Ju B-K, et al. Highly soluble green-emitting Ir(III) complexes with 9-(6-phenyl-pyridin-3-ylmethyl)-9 *H*-carbazole ligands and their application to polymer light-emitting diodes. Journal of Polymer Science Polymer Chemistry Edition 2008;46:7419–28.

[20] Liu H-M, He J, Wang P-F, Xie H-Z, Zhang X-H, Lee C-S, et al. High-efficiency polymer electrophosphorescent diodes based on an Ir(III) complex. Applied Physics Letters 2005;87:221103/1–3.

[21] Zhang X, Chen Z, Yang C, Li Z, Zhang K, Yao H, et al. Highly efficient polymer light-emitting diodes using color-tunable carbazole-based iridium complexes. Chemistry Physics Letters 2006;422:386–90.

[22] Zhang K, Chen Z, Yang C, Zhang X, Tao Y, Duan L, et al. Improving the performance of phosphorescent polymer light-emitting diodes using morphology-stable carbazole-based iridium complexes. Journal of Materials Chemistry 2007;17:3451–60.

[23] Yang C, Zhang X, You H, Zhu L, Chen L, Zhu L, et al. Tuning the energy level, photophysical and electroluminescent properties of heavy metal complexes by controlling the ligation of metal with carbon of carbazole unit. Advanced Functional Materials 2007;17:651–61.

[24] Pai DM, Yanus JF, Stolka M. Trap-controlled hopping transport. Journal of Physical Chemistry 1984;88:4714–7.

[25] Yang XH, Neher D. Polymer electrophosphorescence devices with high power conversion efficiencies. Applied Physics Letters 2004;84:2476–8.

[26] Yang XH, Neher D, Hertel D, Däubler TK. Highly efficient single-layer polymer electrophosphorescent devices. Advanced Materials 2004;16:161–6.